Journal of The Electrochemical Society, **154** (2) P16-P19 (2007)
0013-4651/2006/154(2)/P16/4/$20.00 © The Electrochemical Society

Luminescent Properties and Structure Investigation of $Y_3Al_5O_{12}$/Ce Phosphors with Si Addition

Y. S. Lin, Y. H. Tseng, R. S. Liu,[z] and Jerry C. C. Chan

Department of Chemistry, National Taiwan University, Taipei 106, Taiwan

A new host structure of YAG/Ce phosphor is obtained by the addition of Si in the form of Si_3N_4. The emission spectrum shows blue shift with lower emission intensity due to the changes in coordination environments of the whole crystal structure. Based on the results of ^{27}Al solid-state nuclear magnetic resonance measurements of YAG/Ce + xSi_3N_4, we propose that the Si^{4+} ions are the major substituent into the host structure which is further identified by X-ray diffraction patterns.
 [DOI: 10.1149/1.2405835]

Manuscript submitted October 31, 2005; revised manuscript received October 5, 2006.
Available electronically December 27, 2006.

The white light emitting diode (LED) is an ideal lighting device and its application has been found in many aspects of our daily life, including traffic lights, directional lighting, backlighting for displays, and others.[1] High-luminescent white LED constructed from the blue chip (InGaN) and yellow Ce-doped yttrium aluminate garnet (YAG/Ce) phosphor was first reported by Nakamura and Fasol in 1997.[2] Development of white LEDs using the ultraviolet (UV) chip as the excitation source was also reported[3,4] and this approach is expected to give very high luminescent efficiency. After this work many research groups started to examine the properties of phosphors used in LEDs. Nevertheless, the white LED constructed from the blue chip with yellow YAG phosphors currently remains the most stable and cost-effective system for commercial usage.

In the literature there are two major approaches for the improvement of YAG/Ce phosphors. The first one is to use different synthetic processes to produce YAG/Ce, including sol-gel,[5,6] coprecipitation and heterogeneous precipitation,[7-9] mechanochemical solid reaction,[10,11] pyrolysis,[12] and solvo-thermal methods.[13] Another approach is to add different doping elements into the YAG host[14-16] or to develop different host compositions to investigate the resultant optical properties.[17,18] To date, most of the phosphors used for white LEDs belong to metal–oxide systems which have stable properties for operation and are easy to synthesize. New phosphors with metal-nitride systems as the host structure were reported recently,[19-21] but very little is known about their properties.

In the present work, we added Si_3N_4 into YAG/Ce phosphors to change the host compositions and the luminescent properties. In order to investigate the structural changes caused by the Si_3N_4 addition, ^{27}Al nuclear magnetic resonance (NMR) magic-angle spinning (MAS) spectra and a two-dimensional triple-quantum MAS (TQMAS) spectrum were measured.

Experimental

Preparation of $(Y_{2.95}Ce_{0.05})Al_5O_{12}$.— Precursors $Y(NO_3)_3{\cdot}6H_2O$, $Ce(NO_3)_3{\cdot}6H_2O$, and $Al(NO_3)_3{\cdot}9H_2O$ with the composition of $(Y_{2.95}Ce_{0.05})Al_5O_{12}$ were mixed and ground well in an agate mortar. The mixture was first calcined at 1000°C in air for 24 h. The calcined light-yellow powders were subsequently ground again and sintered in air at 1500°C for 24 h to yield a highly crystalline material. The crystallized powders were then milled and annealed in a reducing atmosphere (5% H_2 in N_2) at 1500°C for 12 h to reduce Ce^{4+} to Ce^{3+}. The final crystalline powders were yellow in color. Firing not only induced the solid-state reaction but also yielded well-crystallized particles with an appropriate mean diameter.

Addition of Si.— Si was added in the form of Si_3O_4 which was mixed into the as-prepared YAG/Ce phosphors with the composition of YAG + xSi_3N_4 (x = 0, 0.2, 0.3, and 0.4). The mixtures were well ground in an agate mortar and sintered in a reducing atmosphere (5% H_2 in N_2) at 1400°C for 5 h.

Characterization.— The crystal structure and phase of the synthesized samples were analyzed using a PANalytical X'Pert PRO X-ray powder diffractometer (XRD) with a wavelength of Cu Kα (λ = 1.5406 Å) at 45 kV and 40 mA. The luminescence spectra were measured using a SPEX Fluorolog-2 spectrometer with a Xe lamp as the light source.

NMR characterization.— All the experiments were carried out on a Bruker DSX-300 spectrometer at ^{27}Al frequency of 78.2 MHz. Isotropic chemical shifts were referenced to 1.0 M aqueous $AlCl_3$. The ^{27}Al TQMAS[22] spectrum was obtained at a spin rate of 12 kHz using the z-filtering sequence.[23] The pulse sequence and coherence-level diagram were shown in Fig. 1. The nutation frequencies of the first two hard pulses and the third soft pulse were 120 and 20 kHz, respectively. Quadrature detection in the F_1 dimension was achieved by the hypercomplex approach. For each t_1 increment 468 transients were accumulated, and a total of 63 increments were done at steps of 83.3 μs. Recycle delay was set to 1 s. Data analyses of the 2D spectra were based on the procedure described earlier.[24] The extracted NMR parameters include the isotropic chemical shift (δ_{iso}) and the second-order quadrupolar effect (χ)

$$\chi = C_Q \sqrt{\left(1 + \frac{\eta_Q^2}{3}\right)}$$

where C_Q is the nuclear quadrupole coupling constant and η_Q is the asymmetry parameter of the electric field gradient tensor at the nuclear site.

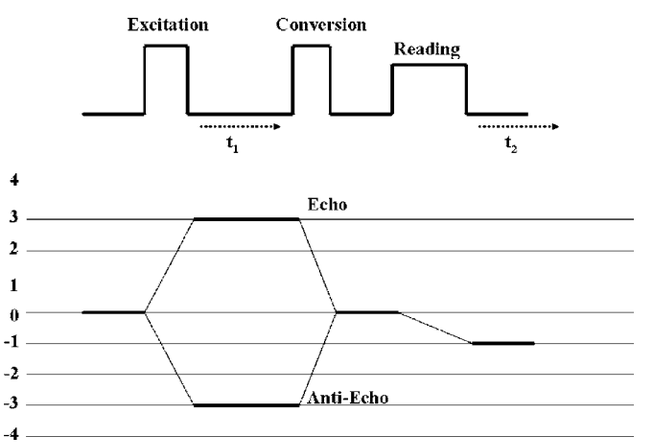

Figure 1. Pulse sequence and coherence level diagram used for recording the ^{27}Al TQMAS NMR spectra.

[z] E-mail: rsliu@ntu.edu.tw

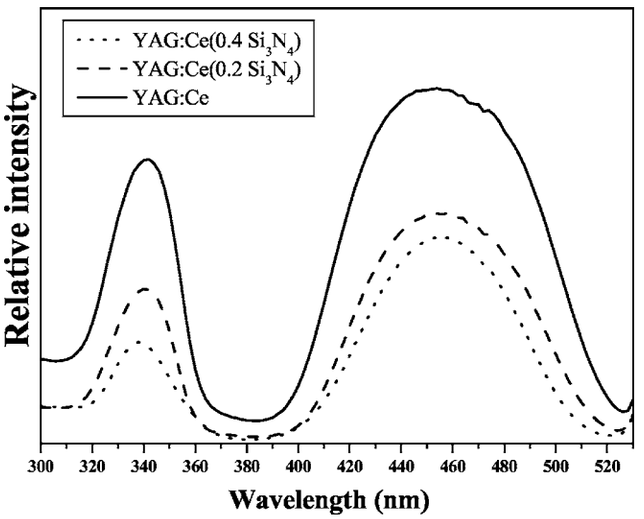

Figure 2. Excitation spectra of $(Y_{2.95}Ce_{0.05})Al_5O_{12}$ with different amounts of Si_3N_4.

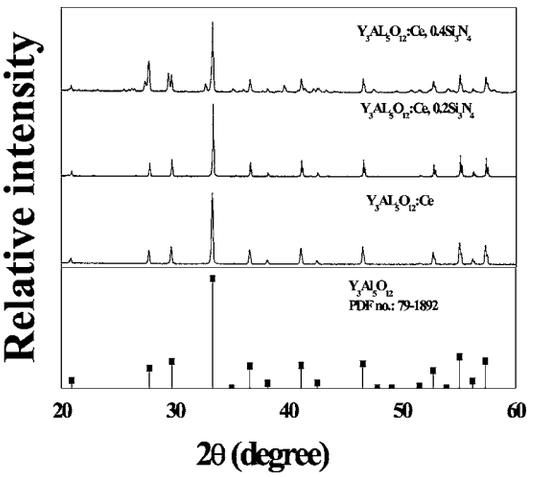

Figure 4. XRD patterns of $(Y_{2.95}Ce_{0.05})Al_5O_{12}$ with different amounts of Si_3N_4. (The standard JCPDS file of $Y_3Al_5O_{12}$/Ce is attached.)

Results and Discussion

Luminescent properties.— Typical excitation spectra of $(Y_{2.95}Ce_{0.05})Al_5O_{12}$ phosphors (monitored at around 530 nm) with different amounts of Si_3N_4 are shown in Fig. 2. All the excitation spectra show two major peaks at about 340 and 465 nm, which are due to the *f-d* transition characteristic of Ce^{3+}. The *d* orbitals of the Ce^{3+} excited states are split into various levels due to the crystal field effects. The lowest two excited states are the ^2B and ^2A states. Figure 2 also shows the variation of intensity with different amounts of Si_3N_4. Referring to the emission spectra (excited at around 460 nm) shown in Fig. 3, the wavelength of the highest emission intensity has a blue shift and the intensities decrease gradually as the amount of Si_3N_4 increases. The ionic character and valence charge of Si^{4+} are so different from those cations of YAG/Ce that the substitution of Si^{4+} may possibly cause the formation of defects in the host. The substitution of atoms in diversity of ionic radius and ionic charge is highly limited on concentration in a presupposition of not changing the major crystal system ($Y_3Al_5O_{12}$ in our experiment).

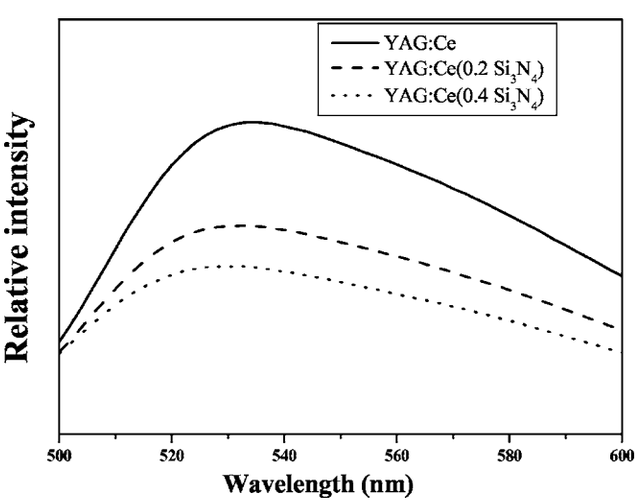

Figure 3. Emission spectra of $(Y_{2.95}Ce_{0.05})Al_5O_{12}$ with different amounts of Si_3N_4.

Some defect vacancies (negative or positive) are formed in crystal with regards to charge balance, which is shown in the following equation

$$4Al^{3+} + 3Si^{4+} \rightarrow V'''_{Al} + 3Si^{\bullet}_{Al}$$

Most defects could be trap centers. Electrons or photons may be transferred into these defect centers and further trapped. They may release energy by nonradiation process but not luminescence and show the quenching effect on spectrum.

The defect formation influences the Ce^{3+} coordination environments. The existence of new elements and defects may influence the crystal field in the crystal. We propose that the substitution of presented synthetic process decreases the covalent character where Ce^{3+} ions feel between coordinated anions. The *f-d* orbital splitting of Ce^{3+} increases, resulting in the observed blue shift. We note in passing that the blue shift is considered to be an advantage for the construction of white LEDs with blue chips at suitable wavelength. In the realization of white LEDs, the different emitted wavelength of the chip must be combined with that of phosphors critically for producing the same white lighting in color. This broadens the ways to combine the blue chip with phosphors when the wavelength varies.

Figure 4 shows the XRD patterns of $(Y_{2.95}Ce_{0.05})Al_5O_{12}$ with different amounts of Si_3N_4. The XRD patterns obtained for all samples correspond to the cubic system with Ia-3d lattice symmetry. Compared with the standard JCPDF files (no. 79-1892 of $Y_3Al_5O_{12}$) the as-synthesized sample with 0.2 molar ratio of Si_3N_4 still shows a pure phase of YAG but an additional phase is found when the molar ratio of Si_3N_4 increases to 0.4. Figure 5 shows the XRD patterns of the as-synthesized samples compared with two crystalline standards of $Y_2Si_2O_7$. It shows that $Y_2Si_2O_7$ is a possible candidate of the new crystalline phase formed due to the Si_3N_4 addition. The ionic radii of the tetra- and hexa-coordinated Si^{4+} ions are 0.26 and 0.4 Å, respectively, while those of tetra-coordinated Al^{3+} and hexa-coordinated Al^{3+} are 0.39 and 0.535 Å, repectively.[25] Consequently, the substitution of the Al^{3+} ions by the Si^{4+} ions would cause the reduction of the lattice parameters, which indeed is what we observed in the XRD data measured for our sample series $(Y_{2.95}Ce_{0.05})Al_5O_{12} + xSi_3N_4$. Figure 6 shows the correlation of the lattice parameters with the amounts of Si_3N_4 added, hence providing partial support for the notion that the Si^{4+} ions, instead of the N^{3-} ions, are the major species substituting the Al^{3+} ions in the host structure in the as-synthesis condition. Therefore, the possible chemical reaction after the addition of Si as the form of Si_3N_4 is

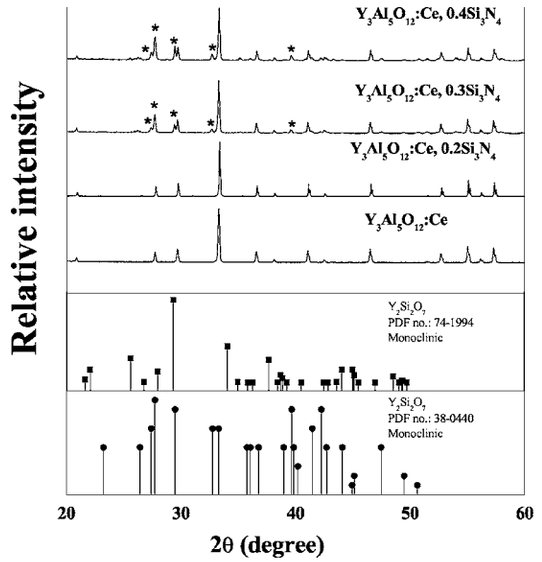

Figure 5. XRD patterns of $(Y_{2.95}Ce_{0.05})Al_5O_{12}$ with different amounts of Si_3N_4 compared with the standards of $Y_2Si_2O_7$.

listed as follows: $Y_3Al_5O_{12} + SiN \rightarrow (Y,Si)_3Al_5O_{12-\delta} + N_2 + Y_2(Si,Al)_2O_{7-\delta}$ (unbalanced chemical equation).

^{27}Al NMR.— We demonstrate in Fig. 2-6 that the addition of Si_3N_4 alters the host lattice and changes the coordination environments of the crystal structure of $(Y_{2.95}Ce_{0.05})Al_5O_{12}$. To understand the influence of the Si_3N_4 addition in more detail, we measured the ^{27}Al NMR spectra for our samples. The spectra shown in Fig. 7 have several overlapping spectral components. To deconvolute the MAS spectra, we measured the two-dimensional TQMAS NMR spectrum of $Y_3Al_5O_{12}$/Ce + 0.4 Si_3N_4. Based on the sheared spectrum shown in Fig. 8, we conclude that there are three major aluminum sites, viz. sites A, B, and C. The extracted NMR parameters are summarized in Table I. The NMR data obtained from the TQMAS spectrum provide reliable initial fitting parameters to the MAS spectra shown in Fig. 7. Note that in the MAS spectra we have identified four different sites. Apparently the site labeled with an asterisk in the MAS spectra, henceforth referred to as an impurity site, has a very small

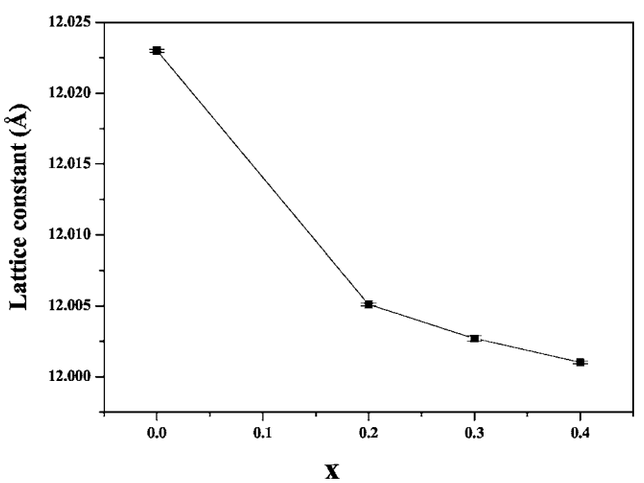

Figure 6. Lattice parameters as a function of x in $(Y_{2.95}Ce_{0.05})Al_5O_{12} + xSi_3N_4$. Here we proposed that x is the amount of Si substituted into YAG in the refinement calculating model.

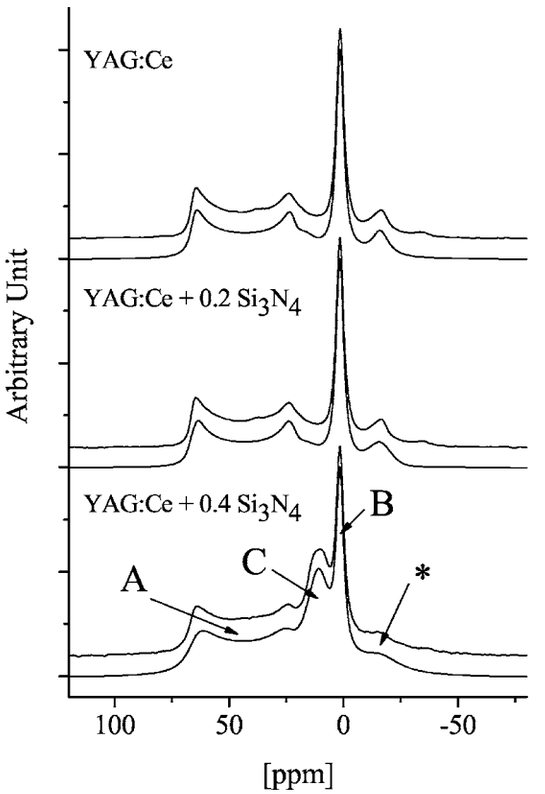

Figure 7. ^{27}Al MAS NMR spectra of $(Y_{2.95}Ce_{0.05})Al_5O_{12}$ with different amounts of Si_3N_4 at 7.0 T.

quadrupolar effect so that it cannot be observed in the TQMAS spectrum. After the so-called Massiot's correction,[26] the relative populations of all the Al sites were obtained (Table I).

Considering the structure of pure $Y_3Al_5O_{12}$, the Al ions occupy two different sites in the crystal lattice and have two coordination numbers. One site is positioned at the center of a tetrahedron (tetra-coordinated Al^{3+}), and the other one is at the center of an octahedron (hexa-coordinated Al^{3+}).[26] The relative population of the tetra-coordinated Al^{3+} and hexa-coordinated Al^{3+} sites are 60 and 40%, respectively. The measured ^{27}Al isotropic chemical shifts and the χ

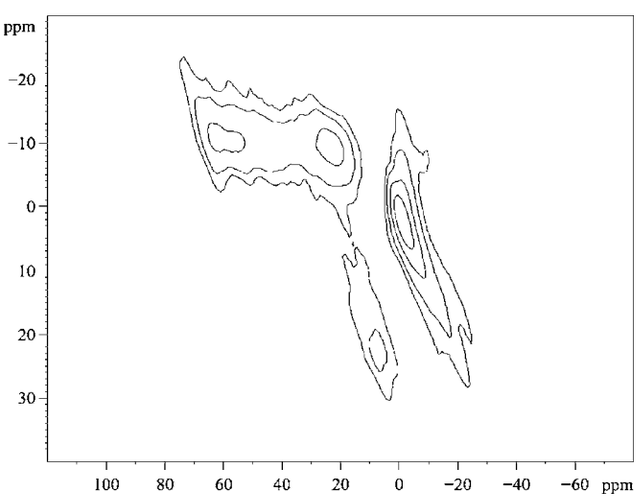

Figure 8. ^{27}Al TQMAS NMR spectra of $(Y_{2.95}Ce_{0.05})Al_5O_{12}$ + 0.4 Si_3N_4.

Table I. Isotropic chemical shift (δ_{iso}), SOQE (MHz), and population percentage parameters for $(Y_{2.95}Ce_{0.05})Al_5O_{12} + xSi_3N_4$ extracted from NMR spectra.

Sample		Site A AlO_4	Site B AlO_6	Site C AlO_6	Impurity phase
YAG/Ce	δ_{iso} (ppm)	78.3	2.6	16.8	−16.0
	SOQE (MHz)	6.0	1.1	--	--
	%	50.6	32.2	7.7	9.5
YAG/Ce	δ_{iso}	78.3	2.6	16.4	−15.8
0.2 Si_3N_4	SOQE	6.0	1.0	--	--
	%	49.6	32.9	9.3	8.2
YAG/Ce	δ_{iso}	77.2	2.9	16.1	−15.5
0.4 Si_3N_4	SOQE	5.8	1.1	2.7	--
	%	42.3	18.4	33.2	6.1

data of sites A and B of our samples are very similar to those reported for $Y_3Al_5O_{12}$.[26] Therefore, sites A and B of our ^{27}Al MAS spectra are readily assigned to tetra-coordinated Al^{3+} and hexa-coordinated Al^{3+}, respectively. Interestingly, the ^{27}Al MAS spectra of the samples $Y_3Al_5O_{12}$/Ce and $Y_3Al_5O_{12}$/Ce + 0.2 Si_3N_4 are very similar, with the population ratios of sites A and B equal to 1.57 and 1.51, respectively. These ratios are very close to the value 1.5 calculated for pure $Y_3Al_5O_{12}$. Therefore, in accordance to the XRD data, the major Al species (sites A and B) of our sample $Y_3Al_5O_{12}$/Ce have the same coordination environments of the tetra-coordinated Al^{3+} and hexa-coordinated Al^{3+} sites of pure $Y_3Al_5O_{12}$. There are two additional Al sites, viz. site C and the impurity phase, which are not found in $Y_3Al_5O_{12}$. Apparently, the doping of Ce^{3+} into $Y_3Al_5O_{12}$ has created a considerable amount of site C and the impurity site, which account for a total of 17.5% of the aluminum sites. These non-$Y_3Al_5O_{12}$ sites were not detected by XRD measurements, showing that they are of amorphous nature or their crystallites may be subnanosized.

For the sample $Y_3Al_5O_{12}$/Ce + 0.4 Si_3N_4, the relative amount of site C increases dramatically, which is accompanied by a significant reduction in the amount of site B. Accordingly, the XRD pattern reveals the formation of a new crystalline phase similar to $Y_2Si_2O_7$. In comparison with the literature data,[26] we assign site C to hexa-coordinated Al^{3+}. We believe that site C arises from the crystalline phase of $Y_2Si_2O_7$. Further analyzing with energy-dispersive spectroscopy, we propose that the possible element ratio in the formula is close to $Y_2(Si_{1.55}Al_{0.45})O_{7-\delta}$. However, the tiny variation in contents between Si and Al elements is unknown considering charge-balance neutrality.

Conclusions

The modification of the host structure of YAG/Ce phosphor is achieved by the addition of Si_3N_4. After the addition of Si_3N_4, emission spectra show a blue shift which is caused by the changes of coordinated environments of the crystal structure. The NMR data reveal the presence of tetra-coordinated Al^{3+} and hexa-coordinated Al^{3+} sites in the $Y_3Al_5O_{12}$ host structure. The substitution of Al^{3+} ions by the Si^{4+} ions causes the formation of a new crystalline phase, which is evidenced by both XRD and NMR measurements.

Acknowledgments

The National Science Council of the Republic of China under grant NSC 94-2113-M-002-030 and The Lite-On Technology Corporation supported this work. We thank C. C. Lin for technical help.

National Science Council of Taiwan assisted in meeting the publication costs of this article.

References

1. G. O. Mueller and R. Mueller-Mach, *Proc. SPIE*, **4776**, 122 (2002).
2. S. Nakamura and G. Fasol, *The Blue Laser Diode*, Springer-Verlag, Berlin (1997).
3. U. Kaufmann, M. Kunzer, K. Köhler, H. Obloh, W. Pletschien, P. Schlotter, R. Schmidt, J. Wagner, A. Ellens, W. Rossner, and M. Kobusch, *Phys. Status Solidi A*, **188**, 143 (2001).
4. J. K. Sheu, S. J. Chang, C. H. Kuo, Y. K. Su, L. W. Wu, Y. C. Lin, W. C. Lai, J. M. Tsai, G. C. Chi, and R. K. Wu, *IEEE Photonics Technol. Lett.*, **15**, 18 (2003).
5. R. V. Kamat, K. T. Pillai, V. N. Vaidya, and D. D. Sood, *Mater. Chem. Phys.*, **46**, 67 (1996).
6. Z. Sun, D. Yuan, H. Li, X. Duan, H. Sun, Z. Wang, Z. Wei, H. Xu, C. Luan, D. Xu, and M. Lv, *J. Alloys Compd.*, **379**, L1 (2004).
7. Y. Pan, M. Wu, and Q. Su, *Mater. Sci. Eng., B*, **106**, 251 (2004).
8. X. Li, H. Liu, J. Wang, X. Zhang, and H. Cui, *Opt. Mater.*, **25**, 407 (2004).
9. F. Yuangli and H. Ryu, *Mater. Sci. Eng., B*, **107**, 14 (2004).
10. J. H. Yum, S. Y. Seo, S. Lee, and Y. E. Sung, *J. Electrochem. Soc.*, **150**, H47 (2003).
11. Q. Zhang and F. Saito, *Powder Technol.*, **129**, 86 (2003).
12. Y. Liu and L. Gao, *J. Am. Chem. Soc.*, **86**, 1651 (2003).
13. X. Li, H. Liu, J. Wang, H. Cui, S. Yang, and I. R. Boughton, *J. Phys. Chem. Solids*, **66**, 201 (2005).
14. C. W. Thiel, H. Cruguel, H. Wu, Y. Sun, C. J. Lapeyre, R. L. Cone, R. W. Equall, and R. M. Macfarlane, *Phys. Rev. B*, **64**, 085107 (2001).
15. R. A. Rodríguez-Rojas, E. De la Rosa-Cruz, L. A. Díaz-Torres, P. Salas, R. Mel éndrez, M. Barboza-Flores, M. A. Meneses-Nava, and O. B. García, *Opt. Mater.*, **25**, 285 (2001).
16. Y. S. Lin, R. S. Liu, and B.-M. Cheng, *J. Electrochem. Soc.*, **152**, J41 (2005).
17. J. K. Park, M. A. Lim, C. H. Lim, H. D. Park, J. T. Park, and S. Y. Choi, *Appl. Phys. Lett.*, **82**, 683 (2003).
18. J. S. Kim, Y. H. Park, S. M. Kim, J. C. Choi, and H. L. Park, *Solid State Commun.*, **133**, 445 (2005).
19. G. Bogner, I. G. Botty, B. Braune, H. T. Hintzen, J. W. H. van Krevel, and G. Waitl, U.S. Pat. 6,649,946 (2003).
20. R.-J. Xie, N. Hirosaki, K. Sakuma, Y. Yamamoto, and M. Mitomo, *Appl. Phys. Lett.*, **84**, 5404 (2004).
21. R.-J. Xie, N. Hirosaki, M. Mitomo, Y. Yamamoto, and T. Suehiro, *J. Phys. Chem. B*, **108**, 12027 (2004).
22. J. P. Amoureux, C. Fernandez, and S. Steuernagel, *J. Magn. Reson., Ser. A*, **A123**, 116 (1993).
23. D. Massiot, C. Bessada, J. P. Coutures, and F. Taulelle, *J. Magn. Reson.*, **90**, 231 (1990).
24. L. Lüchner, J. C. C. Chan, W. M. Warmuth, and H. Eckert, *J. Phys. Chem. B*, **102**, 4495 (1998).
25. R. D. Shannon, *Acta Crystallogr., Sect. A: Cryst. Phys., Diffr., Theor. Gen. Crystallogr.*, **A32**, 751 (1976).
26. P. Florian, M. Gervais, A. Douy, D. Massiot, and J. P. Coutures, *J. Phys. Chem. B*, **105**, 379 (2001).